ELSEVIER

Ceramics International 31 (2005) 677–681

CERAMICS INTERNATIONAL

www.elsevier.com/locate/ceramint

Influence of polyacrylic acid on rheology of SiC suspension and mechanical properties of densified SiC

Xu Hong Wang, Yoshihiro Hirata*

Department of Advanced Nanostructured Materials Science and Technology, Graduate School of Science and Engineering, Kagoshima University, 1-21-40 Korimoto, Kagoshima 890-0065, Japan

Received 23 April 2004; received in revised form 9 June 2004; accepted 21 August 2004
Available online 9 December 2004

Abstract

Addition of polyacrylic acid (PAA) to a 30 vol% SiC suspension with Al_2O_3 (2.5 mass% to SiC) and Y_2O_3 (2.5 mass% to SiC) decreased the viscosity of the suspension at pH 5.0. The prepared suspension was consolidated by filtration through a gypsum mold. The green compact was hot-pressed to 98.7–99.3% theoretical density at 1800 °C under a pressure of 39 MPa for 2 h in an Ar flow. The sintering mechanism was discussed based on the analysis of the shrinkage curve of SiC compacts during the hot-pressing. The grain size of hot-pressed SiC decreased by PAA addition in the suspension. PAA addition improved the Weibull modulus of flexural strength and fracture toughness of SiC at a small expense of average strength. The measured mechanical properties were as follows: average strength 647 MPa, Weibull modulus 6.6, fracture toughness 5.0 MPa $m^{1/2}$ and Vickers hardness 24.5 GPa for the SiC hot-pressed without PAA, and average strength 615 MPa, Weibull modulus 8.2, fracture toughness 5.8 MPa $m^{1/2}$ and Vickers hardness 24.8 GPa for the SiC hot-pressed with PAA.

Keywords: C. Strength; D. Silicon carbide; D. Alumina; D. Yttria; Polyacrylic acid; Colloidal processing; Fracture toughness; Weibull modulus

1. Introduction

Silicon carbide (SiC) is widely useful as a high temperature structural material because of its excellent high temperature strength, good oxidation resistance, high thermal shock resistance, and high hardness. However, it has been impossible to densify a submicrometer-sized SiC powder without sintering additives because of its strong covalent bonding character. Recently the chemical methods for the addition of sintering additives such as Al_2O_3 plus Y_2O_3 to SiC powder have been studied to control the liquid phase sintering and the resultant microstructures of SiC ceramics [1–7]. The densification of Al_2O_3 plus Y_2O_3-doped SiC ceramics proceeds by the liquid phase sintering with a dissolution-precipitation mechanism of SiC in the eutectic liquid of the SiO_2–Al_2O_3–Y_2O_3 system [4,7]. The SiO_2 component forms to a slight extent on the surface of SiC powder. The sinterability of the SiC–Al_2O_3–Y_2O_3 compact depends on the amount and ratio of Al_2O_3–Y_2O_3 system [8,9]. Uniform addition of a small amount of sintering additives to SiC is effective to increase the sinterability. The high dispersion of the Al_2O_3 and Y_2O_3 particles around SiC particles enhances the densification of a consolidated SiC compact. In our previous papers [6,10], we studied the interaction of the submicrometer-sized SiC particles–Al_2O_3 (0.2 μm)–Y_2O_3 (0.1 μm) system in the aqueous suspensions at pH 3–10. The processing in the heterocoagulation region at pH 5 gave the superior properties (high strength, high fracture toughness, and high Weibull modulus) after the hot-pressing of the consolidated powder compacts at 1800 °C. In this paper, addition of a suitable polymer dispersant to the SiC suspension with Al_2O_3 and Y_2O_3 was investigated to enhance the dispersibility of the colloidal particles and to increase the mechanical properties of SiC densified.

* Corresponding author. Tel.: +81 99 285 8325; fax: +81 99 257 4742.
E-mail address: hirata@apc.kagoshima-u.ac.jp (Y. Hirata).

0272-8842/$30.00
doi:10.1016/j.ceramint.2004.08.006

2. Experimental procedure

A following α-SiC powder was used in this experiment: SiC 97.5 mass%, SiO_2 1.75 mass%, C 0.65 mass%, Al 0.025 mass%, Fe 0.027 mass%, median size 0.65 μm (weight standard distribution) and a specific surface area of 13.4 m^2/g (equivalent spherical diameter 0.14 μm, Yakushima Electric Industry Co. Ltd., Kagoshima, Japan). As-received α-SiC powder was mixed with α-Al_2O_3 of a median size 0.2 μm (weight standard distribution) and a specific surface area 10.5 m^2/g (equivalent spherical diameter 0.14 μm, Al_2O_3 > 99.99 mass%, Sumitomo Chemical Industry Co. Ltd., Tokyo, Japan) and Y_2O_3 of a specific surface area 15.0 m^2/g (equivalent spherical diameter 0.08 μm, Y_2O_3 > 99.9 mass%, Shinetsu Chemical Industry Co. Ltd., Tokyo, Japan). The SiC/Al_2O_3/Y_2O_3 (1/0.020/0.016 volume ratio) mixed powders were dispersed at 30 vol% in an aqueous solution at pH 5.0 for 5 h. The pH of each suspension was adjusted using 0.1 M NH_4OH solution. Polyacrylic acid (PAA, average molecular weight 10,000, Daiichi Kogyo Seiyaku Co. Kyoto, Japan) of 0–0.7 mg/m^2 SiC surface was added to the SiC suspension. The rheological properties of the colloidal SiC suspension were measured by a cone and plate type viscometer at room temperature in a shear rate ranging from 1 to 400 s^{-1} (Visconic EMD, EHD type, Tokyo Keiki Co., Tokyo, Japan). The prepared suspension was formed into a rectangular green compact with 38 mm length, 25 mm width and 20 mm height by filtration through gypsum board at room temperature. Bakelite molds were set on a thick flat gypsum board to shape the suspension into the rectangular compact. The consolidated green compacts were hot-pressed under a pressure of 39 MPa at 1800 °C for 2 h in an Ar flow. The heating and cooling rates were 10 °C/min. The density of the hot-pressed compact was measured by the Archimedes method using kerosene. The surface of hot-pressed SiC was polished with 1 μm diamond paste and etched with the mixture of NaCl/NaOH = 85/15 (molar ratio) at 600 °C for 5 min in air to observe the microstructure by scanning electron microscope (SM300, Topcon Technologies Inc., Tokyo, Japan). The hot-pressed SiC was cut into the specimens with sizes of 3 mm height, 4 mm width, and 38 mm length. The specimens were polished with SiC papers of nos. 600 and 2000 and diamond paste of 6 and 1 μm. The Vickers hardness of the hot-pressed SiC was measured at the load of 98 N (Model MVF, Akashi Seisakusho Co. Ltd., Tokyo, Japan). The flexural strength of hot-pressed SiC was measured at room temperature by the four-point flexural method with spans of 30 mm (lower span) and 10 mm (upper span) at a crosshead speed of 0.5 mm/min. The fracture toughness was evaluated by single-edge V-notch beam (SEVNB) method. A thin diamond blade 1 mm thick, where the tip of V-notch had a curvature radius of 20 μm, was used to introduce V-notch of a/W = 0.1–0.6 (a: notch length, W: width of the beam). The strength of the notched specimen was measured by three-point loading over a span 30 mm at a crosshead speed of 0.5 mm/min. Eq. (1) provides the fracture toughness and Eq. (2) indicates the shape factor (Y) of crack at S/W = 7.5. S, P, and B in Eqs. (1) and (2) are the span width, applied load and thickness of beam, respectively.

$$K_{IC} = \frac{3PS}{2BW^2} Y\sqrt{a} \quad (1)$$

$$Y = 1.964 - 2.837\lambda + 13.711\lambda^2 - 23.250\lambda^3 + 24.129\lambda^4,$$

$$\lambda = \frac{a}{W} \quad (2)$$

3. Results and discussion

3.1. Rheology of SiC suspension with PAA

Fig. 1 shows the zeta potentials of SiC, Al_2O_3 and Y_2O_3 particles as a function of suspension pH. The isoelectric points of SiC, Al_2O_3 and Y_2O_3 were pH 2.5, 8.0 and 7.5, respectively. The asymmetry in the zeta potential profile about the isoelectric point for Al_2O_3 and Y_2O_3 revealed that the particle surfaces were charged positively in the acidic conditions below pH 8.0. The pH dependence of the zeta potential of the SiC powder was similar to that of SiO_2 powder, because the surface of SiC particle was coated by thin SiO_2 layers [11–13]. The mixed powder suspension was prepared pH 5.0 (heterocoagulation region between SiC and Al_2O_3 or Y_2O_3). In the SiC–Al_2O_3–Y_2O_3 system at pH 5.0, a part of SiC surface covered with hydroxyls interacts with OH^- ions in the suspension to form the negatively charged sites: $Si–OH + OH^- \rightarrow Si–O^- + H_2O$ [11]. The negatively charged SiC particles are well dispersed by their strong repulsive interaction. On the other hand, some hydroxyls on the surface of Al_2O_3 and Y_2O_3 interact with H^+ ions to form the positively charged sites: $M–OH + H^+ \rightarrow M–OH_2^+$ (M = Al and Y). Positively charged Al_2O_3 and Y_2O_3 particles are adsorbed on the negatively charged SiC particles by their electrostatic attractive forces. The

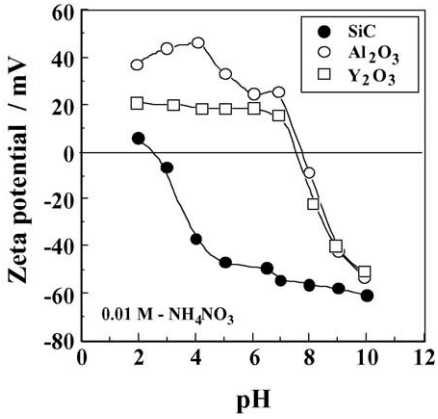

Fig. 1. Zeta potentials of SiC, Al_2O_3 and Y_2O_3 powders as a function of suspension pH.

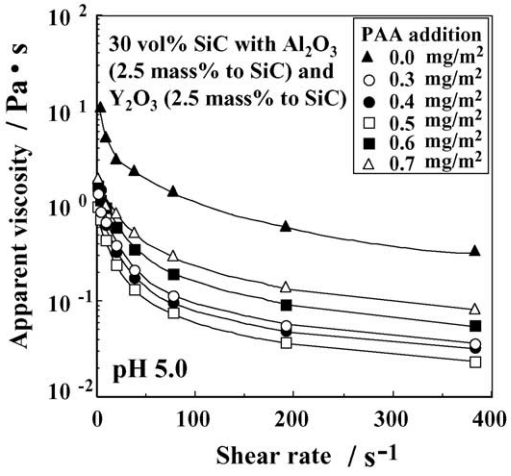

Fig. 2. Effects of addition of PAA on apparent viscosity of SiC suspension with Al_2O_3 and Y_2O_3 at pH 5.0.

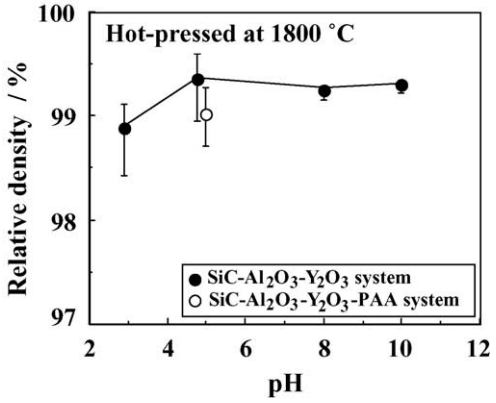

Fig. 3. Relative density of the SiC compact with Al_2O_3, Y_2O_3 and PAA, after hot-pressing at 1800 °C.

heterocoagulation of SiC and Al_2O_3 plus Y_2O_3 shifted the zeta potential of SiC particles from a negative value to a positive value [10]. Furthermore, the important interaction in the SiC–Al_2O_3–Y_2O_3–PAA system at pH 5 are pointed out as follows: (1) PAA [(–CH_2–CH(COOH)–)$_n$] releases H^+ to produce negatively charged polymer at pH higher than 3 [14,15]. The negatively charged PAA is adsorbed on the positively charged $SiOH_2^+$ sites of the thin SiO_2 layer [5]. The number of $SiOH_2^+$ sites is greatly smaller than that of SiO^- sites. (2) Negatively charged PAA is also adsorbed on the Al–OH_2^+ and Y–OH_2^+ sites [15].

Fig. 2 shows the influence of the PAA addition on the apparent viscosity of 30 vol% SiC suspension with Al_2O_3 and Y_2O_3 at pH 5. The mixing of a small amount of Al_2O_3 plus Y_2O_3 particles enhanced the formation of a network structure of heterocoagulated particle clusters in the concentrated SiC suspension, resulting in the increased apparent viscosity [6]. PAA addition decreased the apparent viscosity of the SiC–Al_2O_3–Y_2O_3 suspension, indicating that the dispersibility of the colloidal SiC, Al_2O_3 and Y_2O_3 particles was increased by the adsorption of PAA. The saturated amount of PAA adsorbed was estimated to be 0.5 mg/m^2 because of the minimum apparent viscosity as seen in Fig. 2. The viscosity increased when the amount of PAA added became larger than the saturated amount. This result may be interpreted by the coagulation of the dispersed colloidal particles through free PAA.

3.2. Hot-pressing of SiC

Fig. 3 shows the relative density of SiC hot-pressed at 1800 °C for 2 h under a pressure of 39 MPa as a function of suspension pH. When Al_2O_3 and Y_2O_3 were mixed with SiC, SiO_2 on the surface of SiC interacted with Al_2O_3 and Y_2O_3 to form a liquid phase, whose amount depends on the composition and heating temperature. The composition of SiO_2 (1.75 mass%)–Al_2O_3 (2.5 mass%)–Y_2O_3 (2.5 mass%) in this experiment forms a liquid at 1500 °C in the phase diagram of SiO_2–Al_2O_3–Y_2O_3 system [16–19]. The SiC compacts without PAA were sintered to 98.4–99.6% theoretical density in the wide pH range from 3 to 10. The detailed discussion on this result is reported in our previous paper [10]. PAA addition of the saturated amount to the SiC suspension also provided the high sinterability at 1800 °C. Fig. 4 shows the logarithmic relation between the shrinkage of the SiC compact and heating time after the compact reached the hot-pressing temperature. A good linear relation was observed for both the SiC compacts with and without PAA. In the initial stage of the heating, the slopes were 0.503 and 0.590 for the SiC compacts with and without PAA, respectively. In the final stage of heating, the slopes decreased to 0.186 and 0.188 for the SiC compacts with and without PAA, respectively. The slopes of 0.33, 0.50 and 1.0 represent the early stage sintering mechanism dominated by diffusion in liquid, dissolution–reprecipitation, and viscous deformation, respectively. The experimental result suggests a possibility of the dissolution–reprecipitation mechanism for the early stage of sintering of

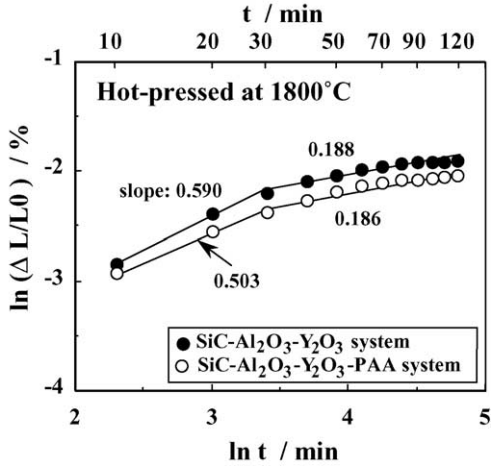

Fig. 4. Logarithmic relation between shrinkage ($\Delta L/L_0$) and hot-pressing time (t) of SiC with Al_2O_3, Y_2O_3 and PAA at 1800 °C.

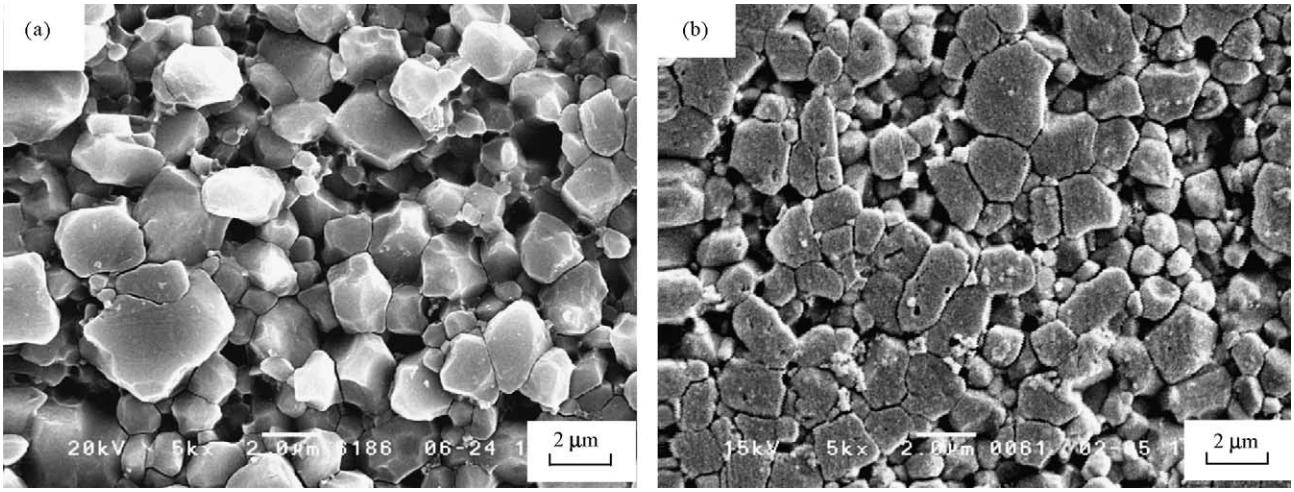

Fig. 5. Microstructures of SiC hot-pressed (a) without and (b) with PAA for 2 h at 1800 °C.

both the SiC compacts in Fig. 4. Fig. 5 shows the microstructures of SiC hot-pressed for 2 h at 1800 °C. Both the microstructures of SiC with and without PAA consisted of the grains of small aspect ratios. The grain size was 0.7–4.9 μm (2.8 μm of average grain size for 200 grains) for the SiC without PAA and 0.6–3.5 μm (2.0 μm of average grain size for 200 grains) for the SiC with PAA. Enhanced dispersion of colloidal particles in the aqueous suspension by PAA addition was effective to achieve the fine SiC microstructure after the densification.

3.2.1. Mechanical properties of densified SiC

Fig. 6 shows the Weibull distribution plots of the flexural strengths for the SiC with and without PAA. The strength at 50% failure probability and Weibull modulus were 647 MPa and 6.6 for the SiC without PAA, and 615 MPa and 8.2 for the SiC with PAA, respectively. The PAA addition improved the Weibull modulus of dense SiC at a small expense of the average strength. Fig. 7 shows the fracture toughness of SiC with and without PAA. PAA addition in the SiC suspension increased the fracture toughness of the hot-pressed SiC (fracture toughness, $K_{IC} = (2E\gamma)^{1/2}$, E: Young's modulus, γ: fracture energy). The Young's modulus of SiC during the flexural strength was 485 GPa for both the SiC with and without PAA. This result suggests that the difference of fracture toughness of SiC compacts with and without PAA reflected the difference of fracture energy. The fracture energy was calculated from the fracture toughness and Young's modulus to be 34.7 and 25.6 J/m^2 for the SiC with and without PAA, respectively. The increased fracture energy of SiC with PAA may be associated with the formation of fine grains (Fig. 5b). The fracture surface of SiC indicates the crack propagation along grain boundaries. Decreased grain size is accompanied by the increase of the grain boundary area. The enhanced branch of main crack along the increased grain boundary area may contribute to the increase of the fracture energy. The fracture energy of SiC with PAA was 36% as high as that of SiC without PAA. On the other hand, the length of grain boundary/m^2 was

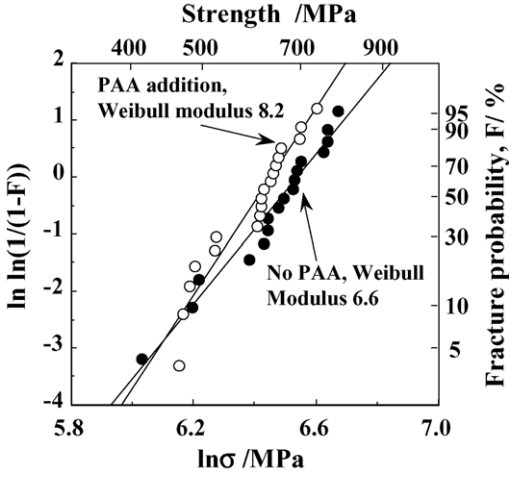

Fig. 6. Weibull distribution plots for flexural strengths of SiC hot-pressed with and without PAA.

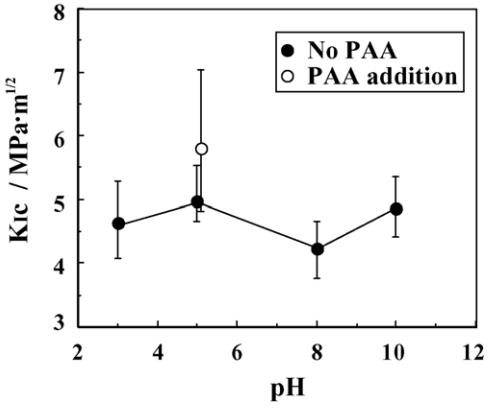

Fig. 7. Fracture toughness of SiC hot-pressed with and without PAA.

calculated on the basis of square grain approximation using the measured average grain sizes. The length of grain boundary for SiC with PAA was 40% as long as that for SiC without PAA. That is, the observed 36% increase in the fracture energy was close to the increase in the length of grain boundary. The Vickers hardness at 98 N of applied load was 24.8 ± 0.65 GPa and 24.5 ± 0.14 GPa for the SiC with and without PAA, respectively. No significant influence of PAA addition was measured on the hardness of SiC. In our previous study, [10] it was found that the hardness of SiC was sensitive to the bulk density and increased at a higher bulk density. In the present experiment, the small difference of the bulk densities for the SiC with and without PAA explains the similar hardness for both the SiC compacts.

4. Conclusions

The apparent viscosity of the SiC–Al_2O_3–Y_2O_3 suspension at pH 5 decreased by PAA addition because of the increased dispersibility of colloidal particles due to the adsorption of PAA.

The SiC compacts with 2 vol% Al_2O_3, 1.6 vol% Y_2O_3 and 0.5 mg/m^2 PAA were hot-pressed to 98.7–99.3% relative density under a pressure of 39 MPa at 1800 °C. A possibility of the dissolution–reprecipitation mechanism was proposed to the early stage of sintering of SiC. Enhanced dispersion of colloidal particles in the aqueous suspension by PAA addition was effective to achieve a fine SiC microstructure after the densification.

PAA addition in the SiC suspension improved the fracture toughness and Weibull modulus of densified SiC.

References

[1] J.H. She, K. Ueno, Densification behavior and mechanical properties of pressureless-sintered silicon carbide ceramics with alumina and yttria additions, Mater. Chem. Phys. 59 (1999) 139–142.
[2] E. Liden, E. Carlstrom, L. Eklund, B. Nyberg, R. Calsson, Homogeneous distribution of sintering additives in liquid-phase sintered silicon carbide, J. Am. Ceram. Soc. 78 (1995) 1761–1768.
[3] Y. Hirata, K. Hidaka, H. Matsumura, Y. Fukushige, S. Sameshima, Colloidal processing and mechanical properties of silicon carbide with alumina, J. Mater. Res. 12 (1997) 3146–3157.
[4] J.H. She, K. Ueno, Effect of additive content on liquid-phase sintering on silicon carbide ceramics, Mater. Res. Bull. 34 (1999) 1629–1636.
[5] Y. Hirata, S. Tabata, J. Ideue, Interactions in the silicon carbide–polyacrylic acid–yttrium ion system, J. Am. Ceram. Soc. 85 (2003) 5–11.
[6] X.H. Wang, R. Shirakawa, Y. Hirata, Y. Hatate, K. Ijichi, Colloidal processing of the SiC–Al_2O_3–Y_2O_3 system, J. Ceram. Proc. Res. 4 (2003) 265–270.
[7] G. Magnani, G.L. Minoccari, L. Pilotti, Flexural strength and toughness of liquid phase sintered silicon carbide, Ceram. Int. 26 (2000) 495–500.
[8] L.M. Wang, W.C. Wei, Colloidal processing and liquid-phase sintering of SiC, J. Ceram. Soc. Jpn. 103 (1995) 434–443.
[9] S.K. Lee, C.H. Kim, Effect of α-SiC versus β-SiC stating powders on microstructure and fracture toughness of SiC sintered with Al_2O_3–Y_2O_3 additives, J. Am. Ceram. Soc. 77 (1994) 1655–1658.
[10] X.H. Wang, Y. Hirata, Colloidal processing and mechanical properties of SiC with Al_2O_3 and Y_2O_3, J. Ceram. Soc. Jpn. 112 (2004) 22–28.
[11] Y. Hirata, K. Miyano, S. Sameshima, Y. Kamino, Reaction between SiC surface and aqueous solutions containing Al ions, Coll. Surf. A 133 (1998) 183–189.
[12] Y. Hirata, S. Nakagama, Y. Ishihara, Dispersion and consolidation of silicon nitride whisker in aqueous suspension, J. Mater. Res. 5 (1990) 640–646.
[13] Y. Hirata, K. Hidaka, Surface characteristics and colloidal processing of silicon carbide, in: H. Yanagida, H. Yoshimura (Eds.), Proceedings of International Symposium on Environmental Issues of Ceramics, The Ceramic Society of Japan, 1995, pp. 264–272.
[14] J. Cesarano III, I.A. Aksay, A. Bleier, Stability of aqueous α-Al_2O_3 suspensions with poly(methacrylic acid) polyelectrolyte, J. Am. Ceram. Soc. 71 (1988) 250–255.
[15] Y. Hirata, T. Kamikakimoto, A. Nishimoto, Y. Ishihara, Interaction between α-alumina surface and polyacrylic acid, J. Ceram. Soc. Jpn. 100 (1992) 7–12.
[16] M.A. Mulla, V.D. Krstic, Low-temperature pressureless sintering of β-silicon carbide with alumina oxide and yttrium oxide additions, Am. Ceram. Soc. Bull. 70 (1991) 439–443.
[17] T. Nagano, K. Kaneko, G.D. Zhom, M. Mitomo, Superplasticity of liquid-phase-sintered β-SiC with Al_2O_3–Y_2O_3–AlN additions in an N_2 atmosphere, J. Am. Ceram. Soc. 83 (2000) 2497–2502.
[18] D. Sciti, A. Bellosi, Effect of additives on densification, microstructure and properties of liquid-phase sintered silicon carbide, J. Mater. Sci. 35 (2000) 3849–3855.
[19] E.M. Levin, C.R. Robbins, H.F. McMurdie, Phase Diagram for Ceramists, The American Ceramic Society, Columbus, OH, 1969 (Fig. 2586).